

Mach-Zehnder Interferometric Biosensor for Point-of-Care Devices

Mrs. Roopa Nanjaiah¹, Mrs. Shwetha M², Ms. Mallika C. S³

¹(Dept. of Electronics and Communication, Sai Vidya Institute of Technology, Bengaluru, India)

^{2,3}(Asst. Prof Dept.of Electronics and Communication, Sai Vidya Institute of Technology, Bengaluru, India)

Abstract: Integrated optical biosensors have become an apparent tool that can be used to detect interactions at the biomolecular level. These biosensors offer advantages like reactivity, dimensions, cost involved in fabrication, manufacturing and ability for multiplexing. Among many, Mach-Zehnder Interferometric biosensor is one such sensor which is generally used in biosensing application as it is a fusion of sensitive mechanisms of waveguide and interferometer. Biosensors displays characteristics like transportability, higher and quicker responsiveness and ease-of-use which helps in utilizing them in real time application like point-of-care devices. Point-of-care testing is a medical diagnosing technique that can be performed when care is needed. This technique is advantageous and can be the substitute for current analysis methodology which is time consuming for the outcome of results. In this work the designing of Mach-Zehnder Interferometer biosensor with rib waveguide structure is considered and the simulation is carried out for the same using COMSOL Multiphysics. The simulation is also carried out to conduct assay on the parameters of waveguide which effects the sensitivity. The Mach-Zehnder interferometers have been previously used for biosensing as they have the highest limit of detection expressed in refractive index units. This helps in observing the engagement of biomolecules in a label-free method.

Keywords: evanescent field, homogeneous sensitivity, optical biosensors, parameter, waveguide

I. Introduction

Sensor is a device which senses the input signal from the surrounding environment and initiates certain activity within the device to give a relevant output. There are optical sensors which are based on the determination and analysis of optical field. The analysis is dealt with phase, distribution of spectra, wavelength are few among others. Biosensors are promising candidates in the technology of optical biosensing as this technology can be a replacement to the established analytical technique because of its easy nature of working, quick responsive nature and also the work carried out using this is cost effective [1].

With the integrated optics there is the development of technology known as lab-on-chip (LOC). This technology incorporates many functionalities including the input light couplers, sensors, micro fluidics and also the output readouts on the same single chip. The conceptual design of LOC includes multidisciplinary fields like biochemistry, opto-electronics microelectronic technology and micro fluids, thus making it suitable for usage in real-time. The size of the chip varies from millimeters to few centimeters. Thus they can be considered in micro system family. LOC finds application in industries like food & beverage and pharmacy, in monitoring environmental conditions, in medical and bio defense field.

The LOC technology helps in development of point-of-care (POC) devices in the health care field. These devices can be used at the bedside when the need of care is required [2]-[4]. In this paper emphasis is on the design and simulation of MZI biosensor with rib waveguide structure that can be used in the development of POC devices in medical field.

II. Optical Biosensors And Its Working

Optical biosensors are the devices which uses principles of optics for converting a biochemical reciprocal action into a relevant output signal. In optical biosensor the principle of detection employed is based on the detection of evanescent field. Usage of evanescent wave grants detection and monitoring the variations in optical parameters due to biomolecular intercommunication. This method is called label-free detection and it is not that appreciable as that of label based detection. However the prerequisites and procedure for this method is more and complex. Thus this method is being replaced by the label-free detection.

Interferometric devices are one among the main type in integrated optical biosensors. These devices works on principle of interferometry, where in superposition of more than one wave results in generating interference patterns. This is only method which provides reference within to take care the variations seen in refractive index. There are several devices in this like the Mach-Zehnder interferometer (MZI), Young Interferometer and others. Among these MZI is the most widely used device because of its high sensitivity. Optical sensors are used with different waveguide structures which helps in propagating the light with very

minimum wastage of input signal. The rib waveguide in particular consists of 3 layers where the top cover and bottom clad encapsulates the core or the film. Due to difference in refractive indices in the layers of the waveguide, within the core total internal reflection (TIR) takes place and causes the incident light to confine within the core. For TIR to happen, the core should have the highest refractive index, the bottom clad to have the next lower value and the cover with least value [5]-[8].

III. Mach-Zehnder Interferometric Biosensor

In MZI the incident light gets divided into two interchangeable beams at the input Y-structure of the MZI waveguide. The beams travel through the arms of MZI identified as reference arm and the sensor arm. After a definite distance beams are again coupled where the arms get connected (output Y-structure) to form a single path. This is shown in the figure 1. A small area on the sensor arm of length L is left open and rest of the area of MZI waveguide is covered with a securing layer. In the sensing arm, the introduced sample reacts and causes variation in the phase. But in reference arm no such changes happen and when combined light is considered at the output, there is an alteration in the phase which induces manipulations in the effective refractive index.

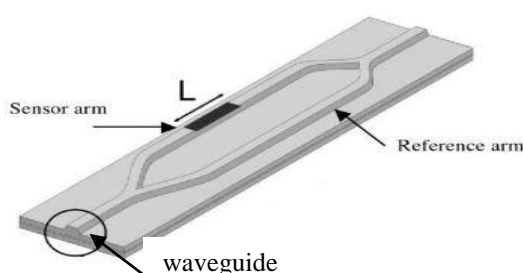


Fig. 1 Configuration of MZI

At the output, the conflict among light from both arms is given by:

$$I \propto [1 + V \cos \Delta\phi] \tag{2.1}$$

where $\Delta\phi = (\phi_r - \phi_s)$ is change in phase observed in the sensor and the reference arm and is given by:

$$\Delta\phi = \frac{2\pi}{\lambda} L \cdot \Delta N \tag{2.2}$$

L is the length in the sensor arm which is opened, ΔN is the effective refractive index and V represents the factor of visibility. The visibility factor helps in designing the Y-structure of MZI with minimum loss [9].

In the sensor arm within the sensor area that is opened, the modulation in phase occur due to the mechanism of evanescent field. When the light pass through waveguide total internal reflection takes place and a part of light that is reflected infiltrate the clad and core interface in the form of electromagnetic field known as the evanescent field. This field of evanescent is around 0.2% of incident light's wavelength. The field exponentially deteriorate in direction of light traversing. Within this evanescent field if any reaction takes place between analyte and receptor results in changing the effective refractive index. This is the criteria for sensing used in biological sensing applications [10]. Figure 2 shows the reaction taking place in the sensor area due to evanescent field.

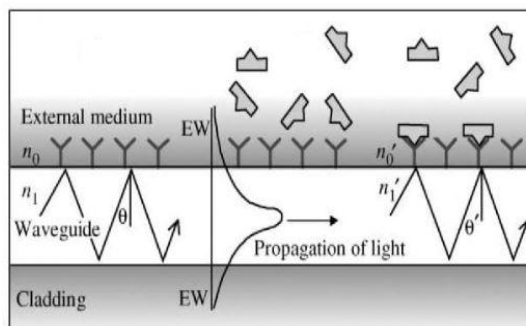


Fig. 2 Evanescent field penetrating the top and bottom layer

IV. Design And Simulation Of Sensor

4.1 Mono-mode behavior

The sensor to be used in application of sensing, should encourage mono-mode behavior along with higher sensitivity. Thus first is to set the dimensions of the waveguide structure which supports mono-mode. The cross section of the rib waveguide whose dimensions has to be optimized is shown in figure 3. The materials taken for simulations is as follows. The undermost cladding layer is of silicon dioxide ($n=1.46$), the cardinal core is of silicon nitride ($n=2$) and top cover medium used is the water ($n=1.33$). The highlighted parameters are 'w' is the rib width, 'h' is the rib height, 't' and 'h' together form the core of the waveguide. n_c , n_f and n_s represents the refractive indices of the three layers cover, film and bottom cladding.

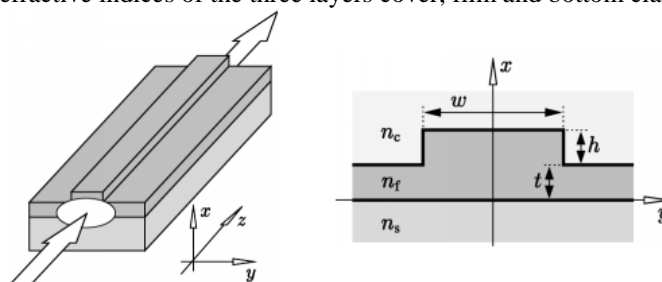


Fig. 3. 3D schematic on left and 2D cross section of rib waveguide on the right side.

When simulated, the mono-mode behavior is obtained even for waveguide structures with smaller rib heights. The mono-mode behavior is considered only for transverse electric (TE) mode. But the confinement of electric field at the core is very less and there is large outspread of field around the core. When simulated for increased rib heights the confinement of electric field towards the core was more than the surrounding interfaces. The simulated results for both the conditions is shown in figure 4 (a) and (b).

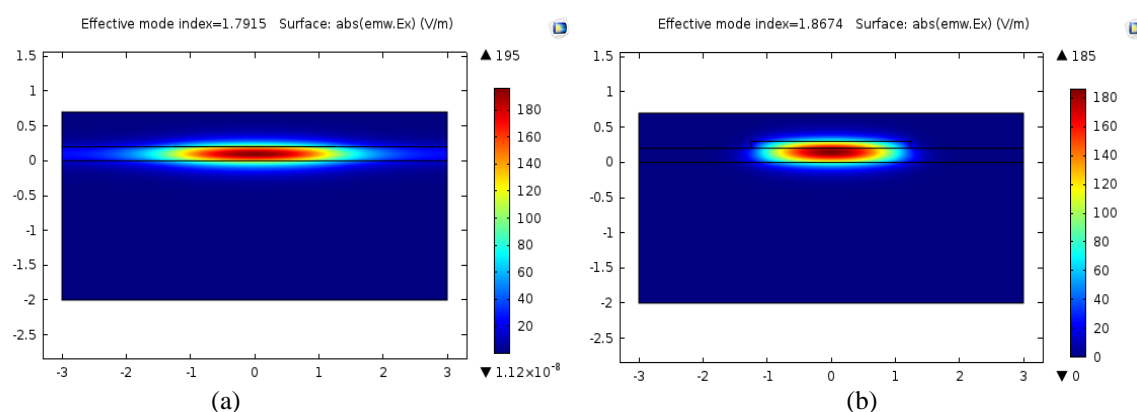


Fig.4 (a) simulation of rib waveguide with smaller rib height of 5nm, (b) simulation of rib waveguide with increased rib height of 75nm.

The sensing principle is based on the decaying evanescent field, which penetrates the core-cladding interface and core-cover medium interface. In these two interfaces core– cover medium is of much importance. Thus waveguides considered here are with rib heights around 45nm-55nm, where in these structures there is confinement of electric field and also spread of field around the core.

It is also possible that by varying the geometrical parameter of the waveguide the mono-mode behavior can be retained. This is obtained by varying core thickness of waveguide and the rib height. The graph in figure 5 shows the dimensions of waveguide which supplements the mono-mode behavior.

The simulation was carried for transverse magnetic (TM) mode. The graph in figure 6 shows the dimensions of both TE and TM mod which gives mono-mode. Comparatively TM mode needs dimensions higher than the TE mode. However the work is restricted with only TE mono-mode.

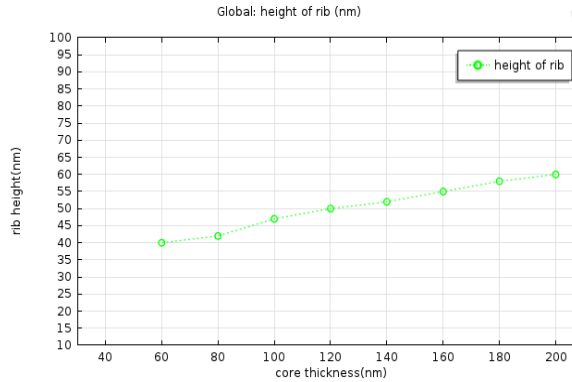


Fig. 5 Dimensions of waveguide parameter which support mono-mode

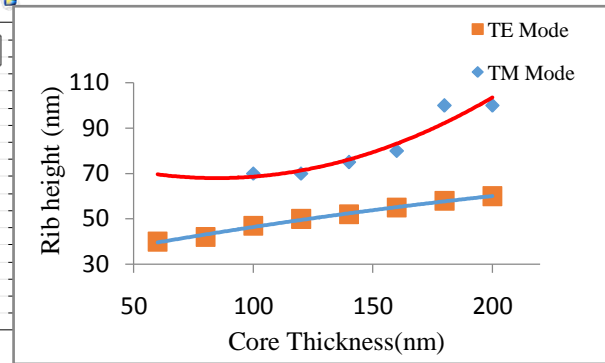


Fig. 6 Dimensions of waveguide parameters for TE0 and TM0 with rib width of 2.5µm

4.2 Sensitivity

Sensitivity is the smallest signal which the device can detect. This is one of the important parameter which describe the performance of the sensor. There are two types known as homogeneous sensitivity and surface sensitivity. In homogeneous sensing, the effective change in index for the mode of propagation is resulted when manipulation of refractive index takes place in the sensitive region. In case of surface sensitivity, the effective change in index for the mode of propagation is resulted when variation in the thickness of a sensitive layer which is laid over the core medium. Usually homogeneous sensitivity finds itself in the detection of concentration of analyte and surface sensitivity used for detection of viruses and bacteria and other biological components considering the aid of receiver molecules which is fixed on the core medium. The simulation work carried out here is restricted to only the homogeneous sensitivity [11]. The homogeneous sensitivity is given by equation (2.3)

$$\frac{dN}{dn} = \frac{P_0}{P_T} * \frac{n}{N} * \left[2 \left(\frac{N}{n} \right)^2 - 1 \right]^\rho \tag{2.3}$$

where $\rho = \begin{cases} 0, & TE \text{ Mode} \\ 1, & TM \text{ Mode} \end{cases}$

Here P_0 is the power in the cover medium, P_T is the total power of the guided mode, n indicates the refractive index of cover medium and N represents the effective refractive index. Since TE mode is considered ρ value is zero. COMSOL is used to compute P_0 , P_T and N. The values introduced into equation (2.3) gives the homogeneous sensitivity. Graph in figure 7 shows the homogeneous sensitivity of the waveguide structure.

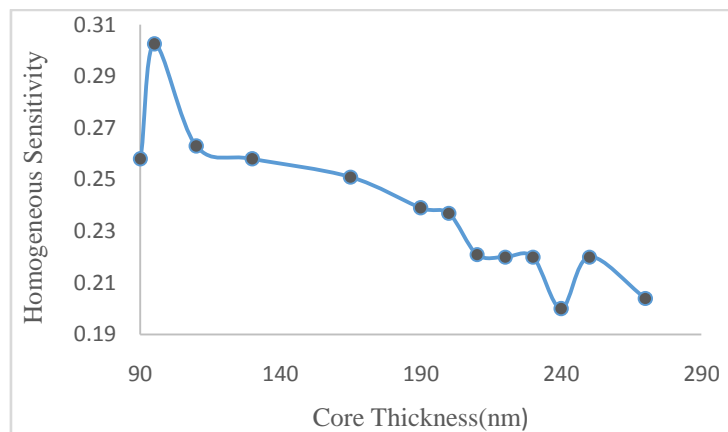


Fig. 7 Core thickness as function of homogeneous sensitivity for TE0

4.2.1 Analysis of homogeneous sensitivity

The variation in the homogeneous sensitivity as function of core thickness, rib height and rib width is seen in this section. As the core thickness is increased the homogeneous sensitivity keeps on decreasing. With smaller core thickness it results in increased effective refractive index and also the spread out of electric field around the core is more which causes the sensitivity to increase. The dimensions of the parameter while performing the simulations were rib width of 2.5µm, rib height as 45nm to 55nm, core thickness varied between 90nm to 300nm and operating wavelength of 633nm. While determining the homogeneous sensitivity the other

parameter of the waveguide like the rib height and rib width is varied. But with varying rib width and rib height the variation of refractive index is very negligible and thus their role in determining the sensitivity is small. This can be observed in the graph in figure 8 as it supplements the result. However the role played by core thickness variation in finding homogeneous sensitivity has greater impact since with varying core thickness the changes observed in effective refractive index is larger (graph resulting this is not shown here). While performing this simulation the core thickness was retained as 200nm and wavelength of 633nm.

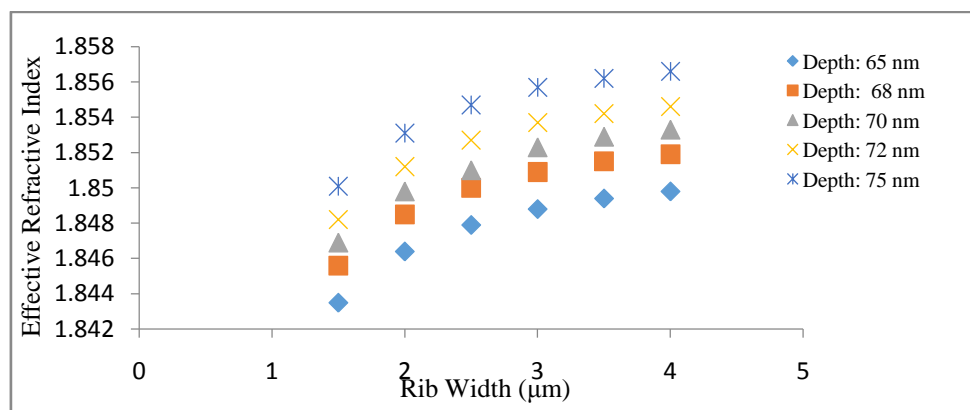


Fig. 8 simulation results for varying rib width and rib height as a function of effective refractive index.

4.3 Evanescent field intensity

Considering evanescent field there is homogeneous sensitivity, where the higher value of evanescent field higher is the sensitivity value. The evanescent field intensity is equivalent to confinement factor Γ_s . This confinement factor is proportional to either the sensitive region or selective region's electric field intensity to overall distribution of mode in guided mode [12]. It is described by equation (2.4)

$$\Gamma_s = \frac{\iint_S |E(x,y)|^2 dx dy}{\iint_{\infty} |E(x,y)|^2 dx dy} \tag{2.4}$$

Along with homogeneous sensitivity evanescent field intensity also helps in optimizing the dimensions of the waveguide structure. Using equation (4) evanescent field intensity value is found using COMSOL. The intensity values were determined for the varying core thickness. Graph is plotted for the same as shown in figure 9.

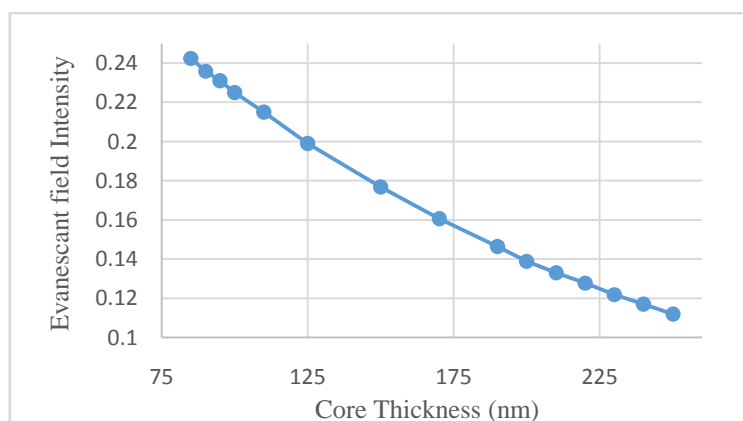


Fig.9 simulation results for variation in evanescent field intensity as a function of core thickness.

4.3.1 Analysis of evanescent field intensity

In this section the evanescent field intensity is evaluated for varying core thickness, rib width and the operating wavelength. From the graph in figure 9 it is observed that, as the core thickness is reduced the intensity value is increased. This represents the condition of higher sensitivity for smaller core thickness. During this simulation of varying core thickness rib width is of 2.5μm and rib height is of 50nm.

Next the rib width variation is done to determine the evanescent field intensity. The core thickness was retained between 90nm to 100nm, rib height of 50nm and wavelength of 633nm. With this condition as the rib width is increased the evanescent field intensity decreases resulting in decreased sensitivity. However with scale down in the rib width the field intensity increases. This graph is shown in figure 10.

Next the analysis is done for evanescent field intensity as function of wavelength. The parameters of the waveguide is retained as seen for previous cases and only the wavelength is varied. The graph representing this condition is shown in figure 11. As seen in graph as the wavelength is reduced the intensity of evanescent field also decreases which results in lessening the sensitivity. The wavelength is varied between 400nm to 700nm.

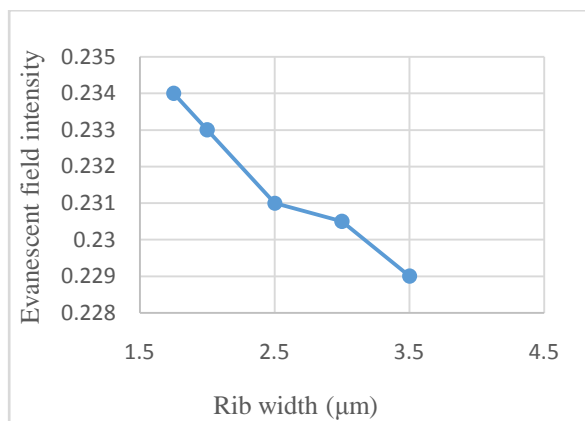


Fig. 10 Evanescent field intensity as a function of rib width

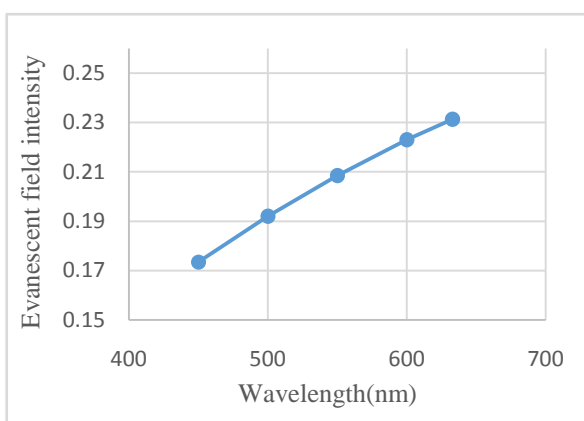


Fig. 11 Evanescent field intensity as function of wavelength.

V. Conclusion

The two conditions considered for sensor design is the mono-mode and sensitivity. With smaller rib height dimension the waveguide structure supports mono-mode but no electric field confinement at core. Thus the increased rib height results in better confinement of the electric field towards the core and also supports mono-mode.

The sensitivity taken into consideration is homogeneous sensitivity since it can be related to the cover medium. When sensitivity is considered, the increased rib height reduces the sensitivity. Thus by reducing the rib height and varying core thickness the dimension of the waveguide structure is obtained which gives maximum sensitivity. To support this condition homogeneous evanescent field intensity is considered whose result also matches stating the lower core thickness with lower rib height gives higher sensitivity. The other parameters which seconds the increased sensitivity are effective refractive index, rib width, rib depth and the operating wavelength. The effective refractive index which is inversely related to homogeneous sensitivity indicates smaller core thickness has higher sensitivity when compared to the rib height and rib width. Considering evanescent field intensity the higher sensitivity is obtained with smaller core thickness, reduced rib width and longer operating wavelength. Thus for the sensor under design to be used in point-of-care devices needs smaller core thickness, smaller rib height and width and longer operating wavelength. When the parameters satisfies these criteria it provides maximum sensitivity.

VI. Future Scope

In the present work only simulation is carried out further for real time implementation the fabrication for the simulated dimensions has to be done. The performance can be evaluated for biological sample as the proposed sensor is for point-of-care diagnostics. Simulation and real time implementation for integration of other components can be checked. This includes the light coupler like the gratings, microfluidics where in the transport of samples and any prerequisite for sample preparation can happen, the output devices where direct readings can be obtained and also electronic system for processing of the signal.

References

- [1] Jose Luis Santos, FaramzrzFarahi, Handbook of Optical Sensors(CRC Press)
- [2] Stefania Dante, Daphne Duval, Ana Belen González Guerrero, Johann Osmond, Kirill Zinoviev, Borja Sepulveda, Carlos Dominguez, Laura M.Lechuga, Towards a complete Lab-On-Chip system using integrated Mach-Zehnder interferometers, Opt.Pura Apl.45(2) 87-95(2012)© Sociedad Española de Óptica
- [3] Michael Ian Lapsley, I.-Kao Chiang, Yue Bing Zheng, Xiaoyun Ding, XiaoleMaoab and Tony Jun Huang, A single-layer, planar, optofluidic Mach-Zehnder interferometer for label-free detection, The Royal Society of Chemistry 2011 Lab Chip, 2011, Lab Chip, 2011, 1795-1800 | 1795
- [4] D. Duvala, A. B. González-Guerreroa, S. Dantea, C. Domínguezb, L. M. Lechuga, Interferometric waveguide biosensors based on Si-technology for point-of-care diagnostic, Silicon Photonics and Photonic Integrated Circuits III, Proc. of SPIE Vol. 8431, 84310P · © 2012 SPIE

- [5] Daphne Duval and Laura M. Lechuga, Nanobiosensors and Bioanalytical Applications Group, CIN2 (CSIC) and CIBER-BBN, Campus UAB, 08193Bellaterra, Barcelona, Spain, Breakthroughs in Photonics 2012: 2012 Breakthroughs in Lab-on-a-Chip and Optical Biosensors, IEEE Photonics Journal DOI: 10.1109/JPHOT.2013.2250943 1943-0655 ©2013 IEEE
- [6] L.M. Lechuga, in: Biosensors and Modern Biospecific Analytical Techniques, Vol.44, edited by L. Gorton
- [7] MoisiXhoxhi, Alma Dudia, AurelYmeti, Interferometric Evanescent Wave Biosensor Principles and Parameters, IOSR Journal of Applied Physics(IOSR-JAP) e-ISSN: 2278-4861. Volume 7, Issue 6 Ver. I (Nov. - Dec. 2015), PP 84-96
- [8] M.-Carmen Estevez, Mar Alvarez and Laura M. Lechuga, Integrated optical devices for lab-on-a-chip biosensing applications, Laser Photonics Rev., 1–25 (2011)/DOI 10.1002/lpor.201100025
- [9] F. Prieto, B. Sepulveda, A. Calle, A. Llobera, C. Dominguez and L.M. Lechuga, Integrated Optical Interferometric Biosensors based on Microelectronics Technology for Biosensing Applications, III CongresoIberoamericano de Sensores y Biosensores
- [10] AlkaVerma, Y. Prajapati, S. Ayub, J.P. Saini, V. Singh, Analytical analysis of sensitivity of optical waveguide sensor, International Journal of Engineering, Science and Technology Vol. 3, No. 3, 2011, pp. 36-40
- [11] S. M. Lindecrantz, J.-C. Tinguely, B. Singh Ahluwalia, O. G. Helleso, Characterization of a waveguide Mach-Zehnder interferometer using PDMS as a cover layer, J. Eur. Opt. Soc.-Rapid 10, 15020 (2015), ISSN 1990-2573
- [12] Dengpeng Yuan, Ying Dong, Yujin Liu and Tianjian Li , Mach-Zehnder Interferometer Biochemical Sensor Based on Silicon-on-Insulator Rib Waveguide with Large Cross Section, Sensors 2015, 15, 21500-21517; doi:10.3390/s150921500.